

IJEAST

INTERNATIONAL JOURNAL
OF ENGINEERING APPLIED SCIENCE
AND TECHNOLOGY

VOLUME : 1 ISSUE : 6 Print / Issue Publication Date: 09-Oct-2016

ISSN : 2455-2143

Indexed In

Google SCHOLAR OPEN ACCESS doi Crossref

WWW.IJEAST.COM

editor@ijeast.com

International Journal of Engineering Applied Sciences and Technology, 2016
Vol. 1, Issue 6, ISSN No. 2455-2143, Pages 52-62
Published Online April - May 2016 in IJEAST (http://www.ijeast.com)



SORET AND RADIATION EFFECTS ON UNSTEADY MHD HEAT AND MASS TRANSFER FLOW OVER A STRETCHING SURFACE EMBEDDED IN A NON-DARCY POROUS MEDIUM

Kalyani Ch
Department of Applied Mathematics
Sri Padmavati Mahila University
Tirupati, India

Sreelakshmi K
Department of Applied Mathematics
Sri Padmavati Mahila University
Tirupati, India

Sarojamma G
Department of Applied Mathematics
Sri Padmavati Mahila University
Tirupati, India

Abstract— **In this paper an analysis has been made to study the characteristics of heat and mass transfer in a non-Darcy flow induced due to a vertical permeable stretching surface embedded in a fluid saturated porous medium in the presence of thermal radiation and viscous dissipation taking the Soret effect and wall slip into account. Similarity variables have been employed to transform the governing non-linear boundary layer equations into a set of non-linear ordinary differential equations. Numerical solutions are obtained for the velocity, temperature and concentration using shooting method and Runge - Kutta method. Comparison of our results under limiting cases is made earlier published results. The influence of the parameters inertial parameter, magnetic parameter, porous parameter, electric field parameter, Prandtl number, thermal radiation parameter, Eckert number heat source/sink parameter, Schmidt number, Soret number, chemical reaction parameter, velocity slip parameter and suction/injection parameter.**

Keywords— ***Non- Darcy porous medium, Soret effect, viscous dissipation, Thermal radiation, Wall slip***

I. INTRODUCTION

The boundary layer flow on a moving continuous surface is frequently encountered in a number of manufacturing processes for example aerodynamic extrusion of plastic films, manufacture of glass filaments, extrusion of polymer sheets from a dye possess the properties of moving continuous surfaces. The MHD flow of an electrically conducting fluid gained significance in manufacturing industries as several metallurgical processes involve the cooling of continuous filaments or strips. When these filaments are drawn through an electrically conducting fluid, the rate of cooling can be controlled in the presence of magnetic field. The study of heat transfer and flow field is essential in the determination of the quality of the final products of such processes as explained by Karwe and Jaluria (1991). Study of heat transfer in flows through porous media find applications in the removal of heat from nuclear fuel debris, radiative waste material disposal, storage of food, transpiration cooling, control of pollutant spread in ground water etc.

At higher rates of flow in a porous medium the inertia effect becomes significant and hence the flow shows a non-Darcy behavior. This non-Darcy behavior is represented through the addition of velocity squared term in the momentum equation, known as the Forchheimer extension. Sing and Tewari (1993) examined the non-Dary free convection flow from vertical surfaces in thermally stratified porous media. Murthy et al. (2013) studied the flow, heat and mass transfer in a nano fluid flow from a vertical plate embedded in a non-Darcy porous medium under convective boundary condition.

Soret effect is referred to the mass transfer induced by temperature gradients. The principle of Soret effect has been used for separation of isotopes and in mixture of gases with very light to moderate molecular weight. In many studies the Soret effect is neglected considering that its effect is of a smaller order of magnitude than the effect described by Fick's law. However, this effect cannot be neglected as it is found that the flow field in a mixed convective boundary layer over a vertical surface through a porous medium is influenced appreciably by the Soret effect.

Vempati and Laxmi-Narayana-Gari (2010) studied the double diffusive effects on the unsteady MHD flow of an electrically conducting, viscous and incompressible fluid over an infinite flat plate under oscillatory suction and thermal radiation. Reddy and Reddy (2010) discussed the double diffusive effects on the flow past an infinite moving plate through a

International Journal of Engineering Applied Sciences and Technology, 2016
Vol. 1, Issue 6, ISSN No. 2455-2143, Pages 52-62
Published Online April - May 2016 in IJEAST (http://www.ijeast.com)

porous medium with viscous heating. Dulal Pal and Mondal (2012) studied heat and mass transfer characteristics of the flow over a stretching surface through a porous medium considering ,Soret and Dufour effects in the presence of electrical field and non-uniform heat source/sink. In a subsequent study (2012) they examined the MHD non-Darcy mixed convective flow due to a stretching surface embedded in a porous medium considering the effect of temperature dependent viscosity and non uniform heat source/ sink and electrical field.

In this paper we study the effect of Soret and thermal radiation MHD non-Darcy flow of an incompressible electrically conducting fluid induced by a permeable stretching surface in the presence of viscous heating and heat source/sink.

II. MATHEMATICAL FORMULATION

Consider the non-Darcy steady mixed convective heat and mass transfer of viscous incompressible and electrically conducting fluid flow induced by a vertical stretching sheet embedded in a fluid saturated porous medium with the plane $y = 0$ of a coordinate system as shown in Fig. 1.

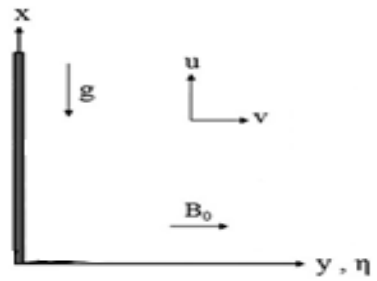


Fig. 1 Physical model and coordinate system

The flow region is subjected to a uniform transverse magnetic field $\vec{B} = (0, B_0, 0)$ and uniform electric field $\vec{E} = (0, 0, -E_0)$. It is assumed that the flow is generated by stretching of an elastic boundary sheet by imposing two equal and opposite forces in such a way that velocity of the boundary sheet is of linear order of the flow direction. The Maxwell's equations are $\nabla \cdot \vec{B} = 0$ and $\nabla \times \vec{E} = 0$. From the Ohm's law is $\vec{J} = \sigma(\vec{E} + \vec{q} \square \vec{B})$, where $\vec{J}$ is the Joule current, σ is the magnetic permeability and $\vec{q}$ is the fluid velocity. The induced magnetic field due to the motion of electrically conducting fluid is negligible. The temperature and the species concentration have quadratic variations with the distance from the origin. The fluid properties are assumed to be constant except the density in the buoyancy terms of the linear momentum equation which is approximated according to Boussinesq's approximation. Thus the governing equations are given by

$$\frac{\partial u}{\partial x} + \frac{\partial v}{\partial y} = 0 \tag{1}$$

$$\frac{1}{\varepsilon^2}\left(u\frac{\partial u}{\partial x} + v\frac{\partial u}{\partial y}\right) = \frac{\nu}{\varepsilon}\frac{\partial^2 u}{\partial y^2} + \frac{\sigma}{\rho}(E_0 B_0 - B_0^2 u) - \frac{\nu}{k}u - \frac{C_b}{\sqrt{k}}u^2 + g\beta_T(T - T_\infty) \tag{2}$$

$$u\frac{\partial T}{\partial x} + v\frac{\partial T}{\partial y} = \frac{K}{\rho c_p}\frac{\partial^2 T}{\partial y^2} - \frac{1}{\rho c_p}\frac{\partial q_r}{\partial y} + \frac{\mu}{\rho c_p}\left(\frac{\partial u}{\partial y}\right)^2 + \frac{\sigma}{\rho c_p}(uB_0 - E_0)^2 + \frac{Q}{\rho c_p}(T - T_\infty) \tag{3}$$

$$u\frac{\partial C}{\partial x} + v\frac{\partial C}{\partial y} = D_m\frac{\partial^2 C}{\partial y^2} + \frac{D_m k_T}{T_m}\frac{\partial^2 T}{\partial y^2} - K_1(C - C_\infty) \tag{4}$$

where u and v are the fluid velocity components along x and y axes, respectively, ε is the porosity of the medium, ν is the kinematic viscosity, ρ is the density of the fluid, σ is the electrical conductivity, E_0 is the electric field strength in the transverse direction, B_0 is the transverse magnetic field strength, k is the permeability of porous medium, C_b is the form of drag coefficient which is independent of viscosity and other physical properties of the fluid which depend on the geometry of the medium, g is the acceleration due to gravity, β_T is the coefficient of thermal expansion, T is the temperature of the fluid inside the thermal boundary layer, T_w is the uniform temperature and T_∞ is the fluid temperature in the free stream with $T_w > T_\infty$, C is the fluid concentration, C_w is the uniform concentration and C_∞ is the fluid concentration in the free stream with $C_w > C_\infty$, c_p is the specific heat at constant pressure, μ is the dynamic viscocity of the fluid, q_r is the radiative heat flux, K is the thermal conductivity of the medium, Q is the uniform volumetric heat absorption, D_m is the mass diffusivity, T_m is the mean fluid temperature, k_T is the thermal-diffusion ratio, K_1 is the chemical reaction.

By using Rosseland approximation, the radiative heat flux is given by

$$q_r = -\frac{4\sigma^*}{3k^*}\frac{\partial T^4}{\partial y} \tag{5}$$

Where σ^* is the Stefen-Boltzman constant and k^* is the absorption coefficient.

T^4 may be linearly expanded in a Taylor's series about T_∞ to get

$$T^4 = T_\infty^4 + 4T_\infty^3(T - T_\infty) + 6T_\infty^2(T - T_\infty)^2 + \cdots,$$

and neglecting higher order terms beyond the first degree in $(T - T_\infty)$,

we obtain $T^4 \cong 4T_\infty^3\, T - 3T_\infty^4$ (6)

Boundary conditions:

$$u = u_w(x) + N\nu\frac{\partial u}{\partial y},\ v = v_w, T = T_w = T_\infty + A_0\left(\frac{x}{l}\right)^2$$
$$C = C_w = C_\infty + A_1\left(\frac{x}{l}\right)^2 \qquad at\ y = 0,$$
$$u \to 0,\quad T \to T_\infty,\quad C \to C_\infty \quad as\ y \to \infty \tag{7}$$

Where $u_w(x) = bx$ is the velocity of the stretching surface, b is the proportionality constant of the stretching velocity, N is the velocity slip factor which changes with time, $v_w = -(\nu \mathrm{u_w}/x)^{1/2}$fw represent the mass transfer velocity at the surface of the sheet with $v_w > 0$ for injection (blowing) and $v_w < 0$ for blowing (suction), and $v_w = 0$ corresponds to an impermeable sheet, A_0 is the parameter of temperature distribution on the stretching surface, A_1 is the parameter of concentration distribution on the stretching surface.

International Journal of Engineering Applied Sciences and Technology, 2016
Vol. 1, Issue 6, ISSN No. 2455-2143, Pages 52-62
Published Online April - May 2016 in IJEAST (http://www.ijeast.com)

To solve the governing boundary layer equations (2) – (4), the following similarity transformations are introduced:

$$u = bxf'(\eta), v = -\sqrt{bv}f(\eta),\ \eta = \sqrt{\frac{b}{v}}y$$
$$\theta(\eta) = \frac{T-T_\infty}{T_w-T_\infty},\quad \phi(\eta) = \frac{C-C_\infty}{C_w-C_\infty} \tag{8}$$

Substitution of equation (8) into the governing equations (2) – (4) and using the above relations we finally obtain a system of non-linear ordinary differential equations with appropriate boundary conditions

$$\frac{f'''}{\varepsilon} + \frac{ff''}{\varepsilon^2} - \frac{f'^2}{\varepsilon^2} + M(E_1 - f') - F^* f'^2 + Gr\theta - k_1 f' = 0 \tag{9}$$
$$\left(1+\frac{4}{3}Nr\right)\theta'' + P_r[f\theta' - 2f'\theta + MEc(E_1 - f')^2 + Ec(f'')^2 + \delta\theta] = 0 \tag{10}$$
$$\phi'' + Sc(f\,\phi' - 2f'\,\phi - \gamma\phi + Sr\,\theta'') = 0 \tag{11}$$

The boundary condition (7) becomes:

$$f(0) = fw,\ f'(0) = 1 + \mathrm{hf}''(0),$$
$$\theta(0) = 1,\ \phi(0) = 1 \qquad at\ \eta = 0 \tag{12}$$
$$f'(\infty) = 0,\ \theta(\infty) = 0,\ \phi(\infty) = 0\ as\ \eta\to\infty \tag{13}$$

Where primes denote differentiation with respect to η, $M = \sigma B_0^2/\rho b$ is the magnetic parameter, $k_1 = \nu/kb$ is the porous parameter, $E_1 = E_0/B_0 bx$ is the electric field parameter, $F^* = C_b x/\sqrt{k}$ is the inertial parameter, $Gr = g\beta_T(T_w - T_\infty)/b^2 x$ is the buoyancy or mixed convection parameter, $Pr = \rho c_p \nu/K$ is the Prandtl number, $Nr = 4\sigma^* T_\infty^3/Kk^*$ is the thermal radiation parameter, $E_c = b^2\, l^2/c_p A_0$ is the Eckert number, $\delta = Q/b\rho c_p$ is the heat source/sink parameter, $Sc = \nu/D_m$ is the Schmidt number, $\gamma = K_1/b$ is the chemical reaction parameter, $Sr = \frac{D_m k_T(T_w-T_\infty)}{\nu T_m(C_w-C_\infty)}$ is the Soret number and $h = N\sqrt{bv}$ is the velocity slip parameter.

The physical quantities of engineering interest in this problem are the skin friction coefficientC_f, which is defined as

$$C_f = \frac{2\tau_w}{\rho u_w^2} \tag{14}$$

Where the wall shear stress τ_w is given by

$$\tau_w = \mu\left(\frac{\partial u}{\partial y}\right)_{y=0} \tag{15}$$

Using the non-dimensional variables equation (8), we get from equations (14) and (15) as

$$\frac{1}{2}C_f\sqrt{Re_x} = f''(0) \tag{16}$$

The local Nusselt number which is defined as

$$Nu_x = \frac{x\,q_w}{K(T_w-T_\infty)} \tag{17}$$

Where q_w the heat transfer from the sheet is given by

$$q_w = -K\left(\frac{\partial T}{\partial y}\right)_{y=0} \tag{18}$$

Using the non-dimensional variables (8), we get from equations (17) and (18) as

$$Nu_x/Re_x^{1/2} = -\theta'(0) \tag{19}$$

The physical quantity of interest is the local Sherwood number which is defined as

$$Sh_x = \frac{xq_m}{D_m(C_w-C_\infty)} \tag{20}$$

Where q_m is the mass transfer which is defined by

$$q_m = -D_m\left(\frac{\partial C}{\partial y}\right)_{y=0} \tag{21}$$

Using the non-dimensional variables (8), we get from (20) and (21) as

$$Sh_x/Re_x^{1/2} = -\phi'(0) \tag{22}$$

Where $Re_x = \frac{xu_w(x)}{\nu}$ is the local Reynolds number

III. Results and Discussion

In this analysis numerical solutions are obtained to investigate the effect of various governing parameters on non-Darcy convective mass diffusion over a stretching surface in the presence of a magnetic field, electrical field, thermal radiation, joule heating, viscous dissipation and heat source/sink. The non-linear ordinary differential equations are integrated by Runge-Kutta method with shooting technique. The accuracy of this method is established by comparing our results of $-\theta'(0)$ with those obtained by Chen (1998), Grubka and Bobba (1985), Aziz (2010) and Dulal Pal and Mondal (2012) in the absence of buoyancy force, magnetic field, porous medium, viscous dissipation, heat source/sink parameter, thermal radiation and diffusion equation with no slip condition. Table 1 shows that our results are in excellent agreement.

Table -1 Comparison values of $-\theta'(0)$ for M = E_1 = F^* = Gr = k_1 = Nr = Ec = δ = Sc = γ = Sr = fw = h = 0, ε = 1.

Pr	Chen (1998)	Grubka and Bobba (1985)	Aziz (2010)	Dulal Pal and Mondal (2012)	Present results
1.0	1.33334	1.3333	1.33333	1.33333	1.33333
3.0	2.50972	2.5097	2.50971	2.50972	2.50972
7.0	3.97150	-	3.97151	-	3.97151
10	4.79686	4.7969	4.79687	4.79687	4.79686
100	15.7118	15.712	15.7120	-	15.7119

Figs. 2 – 4 illustrate the influence of magnetic parameter on velocity, temperature and species concentration, by considering other physical parameters fixed. Fig. 2 reveals that the effect of magnetic parameter is to diminish the velocity distribution in the boundary layer leading to thinning of the thickness of the boundary layer. This may be attributed to the body force namely Lorentz force developed due to the transverse magnetic field, which opposes the fluid motion. In turn the temperature and concentration of the fluid are observed to increase with increase in M (Figs. 3 & 4). Consequently the thermal and solutal boundary layers are enlarged. The variation of the electric field parameter E_1 on velocity is presented in Fig. 5. It is evident that the electric



parameter increases the velocity distribution throughout the hydrodynamic boundary layer near the boundary. However, a little away from the stretching sheet, the enhancement in the velocity is more pronounced. This shows that the streamlines are drifted away from the surface. We may conclude that the electric force serves as an accelerating force to overcome the frictional resistance. Fig. 6 indicates that the temperature is decreased for an increase in electric field parameter due to increase in the mass flux. The species concentration shows an enhancement for an increase in E_1 (Fig. 7).

The influence of porosity parameter ε of porous medium is plotted in Figs. 8 – 10. For an increase in the value of the porosity parameter the velocity distribution in the fluid flow increases while a reduction in temperature and concentration is observed. A similar behavior in concentration is observed by Dulal Pal and Mondal (2012).

Figs. 11 – 13 depict the influence of inertial parameter (F^*) on the velocity, temperature and concentration. Fig. 11 reveals that the velocity gets diminished with increase in the value of drag coefficient while a reversal trend in the temperature and concentration is seen.

Figs. 14 – 16 represent the variations of velocity, temperature and concentration distribution in the boundary layer for different values of the buoyancy parameter Gr. It is seen that the velocity increases with increase in the thermal buoyancy parameter Gr as the thermal buoyancy force acts as a favorable pressure gradient accelerating the fluid flow in the boundary layer. However, increasing values of Gr drop the temperature and concentration resulting in the reduction in the thickness of the thermal and solutal boundary layers.

Fig. 17 indicates that the velocity distribution shows a decreasing tendency with increasing values of the porous permeability parameter as expected k_1 as expected and hence velocities are reduced. Since increasing values of k_1 correspond to decreasing permeability of the medium. Consequently the temperature and concentration distributions increased (Figs. 18 and 19).

Fig. 20 depicts that the Prandtl number has a decreasing influence on the temperature throughout the thermal boundary layer as increasing values of Pr imply smaller rate of thermal diffusion.

Fig. 21 indicates the variation of thermal radiation parameter on temperature. Higher values of Nr correspond to enhanced radiation and consequently the temperatures are increased.

Fig. 22 depicts that increased values of Eckert number enhance the temperature due to the release of stored energy owing to frictional heating. When Ec assumes values greater than two, an over shoot above the prescribed value of the surface temperature occurs on the boundary.

Fig. 23 illustrates the effects of heat source/sink on temperature. A positive value of δ implies that a heat source is present in the fluid which releases energy. As δ increases more energy shall be released and thus the fluid becomes hotter giving rise to a higher a temperature. When δ is negative it corresponds to a heat sink in which case energy is absorbed and hence there is a reduction in the temperature. For increasing values of the sink parameter the temperature further decreases.

Fig. 24 shows that the Schmidt's number decreases the concentration as expected and hence the thickness of the solutal boundary layer is reduced for higher values of Sc. Fig. 25 reveals that the concentration distribution enhances appreciably with increasing values of Soret number.

The effect of chemical reaction on concentration distribution is plotted in Fig. 26. The concentration from its higher value that is unity on the boundary starts descending till it attains the minimum value of zero at far infinity. As the chemical reaction parameter takes larger values, we observe that the concentration decreases further. This may be attributed to the fact that destructive chemical reduces the solutal boundary layer thickness and contributes the rate of mass transfer.

Fig. 27 shows the effect of surface mass transfer on velocity. It is observed that as the injection ($fw < 0$) rate increases the fluid velocity increases. A reversal behavior is noticed for increase in suction rate ($fw > 0$) as expected. The temperature and concentration are found to decrease with suction and an opposite effect with injection (Figs. 28 and 29).

Figs. 30 – 32 draw the influence of velocity slip parameter (h) on velocity, temperature and species concentration. The effect of velocity slip parameter on velocity is found to reduce while it enhances the temperature and concentration.

Table 2 gives the values of surface shear stress, Nusselt number and Sherwood number. It is observed that when the magnetic field parameter assumes higher values the absolute values of surface drag coefficient decrease with a reduction in the rate of heat and mass transfer. The electric field parameter is seen to enhance the drag coefficient, Nusselt number and Sherwood number. The inertial parameter is observed to have a decreasing influence on surface drag coefficient and increases the rate of heat and mass transfer. The buoyancy parameter Gr is seen to increase the values of skin friction, Nusselt number and Sherwood number. The permeability parameter (k_1) reduces the drag coefficient, Nusselt number and Sherwood number. It is observed that the surface drag coefficient and Nusselt number of fluids with higher Prandtl number are higher than the low Prandtl number fluids while an opposite behavior in Sherwood number is noticed. As Nr varies from 0.5 to 2.0 Nusselt number is in the range 1.524504 – 0.842404. When Ec enhances from 1 to 4 the rate of heat transfer is found to increase by 53.41%. The effect of heat source/sink parameter is found is seen to increase rate of heat transfer. The Schmidt number and chemical reaction parameter have a reducing effect on drag coefficient, Nusselt number and a reverse effect on Sherwood number. Increasing values of Soret number are seen to increase the skin friction coefficient and Nusselt number while Sherwood number decreases. As velocity slip parameter varies from 0.1 to 0.4 the rate of heat transfer is enhanced by 3.15% and rate of mass transfer by 3.12% and the surface drag coefficient is increased by 32.08%.

International Journal of Engineering Applied Sciences and Technology, 2016
Vol. 1, Issue 6, ISSN No. 2455-2143, Pages 52-62
Published Online April - May 2016 in IJEAST (http://www.ijeast.com)

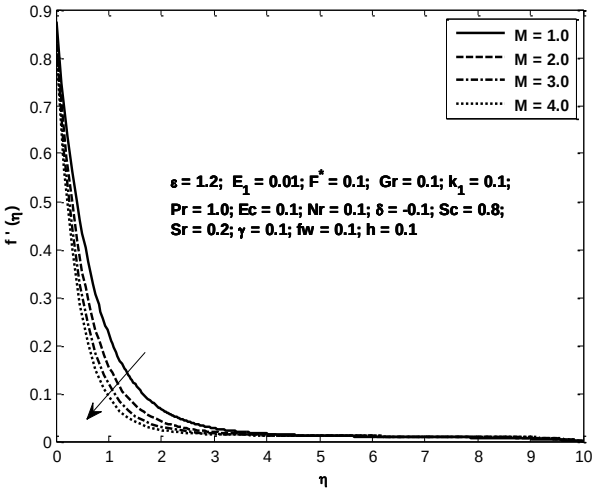


Fig. 2: Velocity profiles for different Values of M

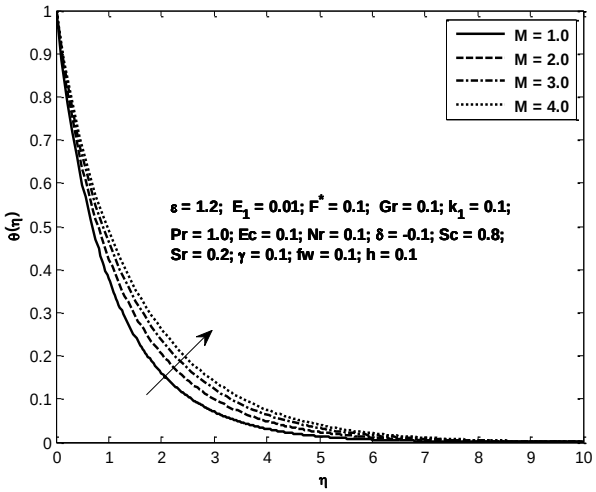


Fig. 3: Temperature profiles for different values of M

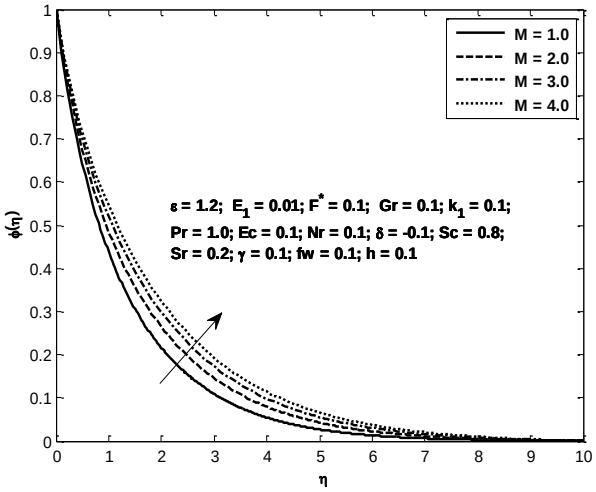


Fig. 4: Concentration profiles for different values of M

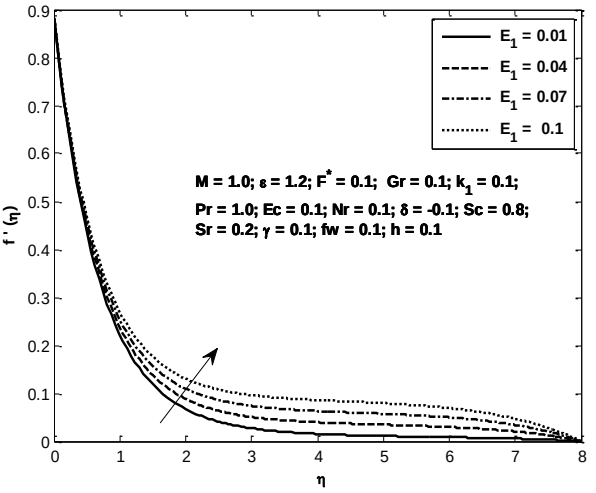


Fig. 5: Velocity profiles for different Values of E_1

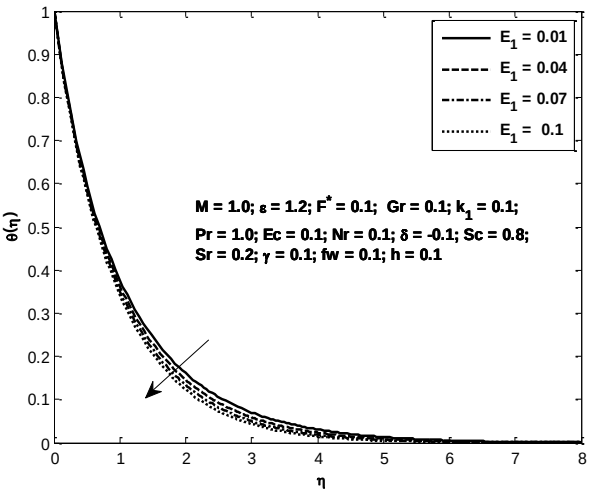


Fig. 6: Temperature profiles for different values of E_1

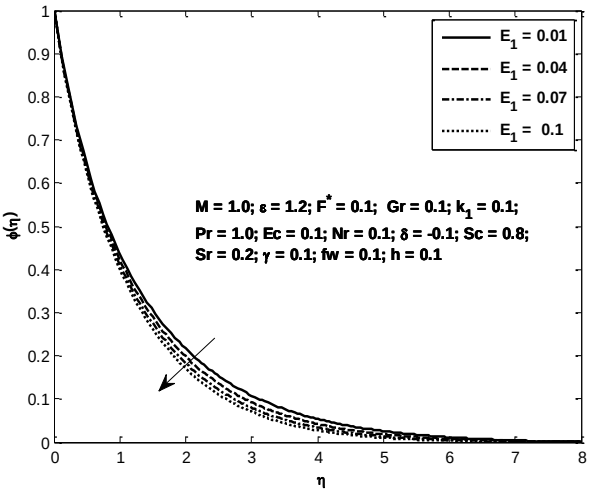


Fig. 7: Concentration profiles for different values of E_1

International Journal of Engineering Applied Sciences and Technology, 2016
Vol. 1, Issue 6, ISSN No. 2455-2143, Pages 52-62
Published Online April - May 2016 in IJEAST (http://www.ijeast.com)

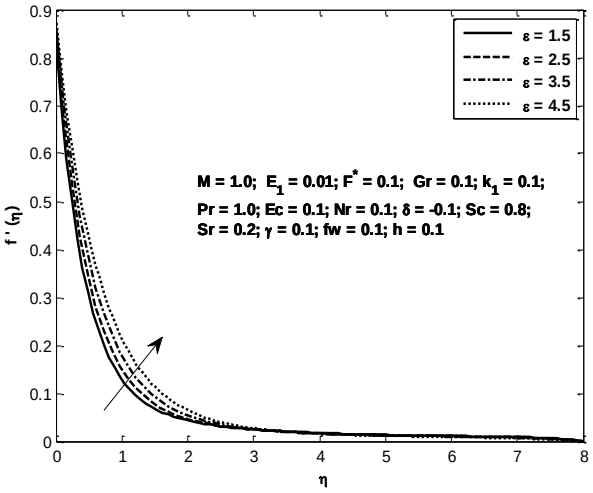


Fig. 8: Velocity profiles for different Values of ε

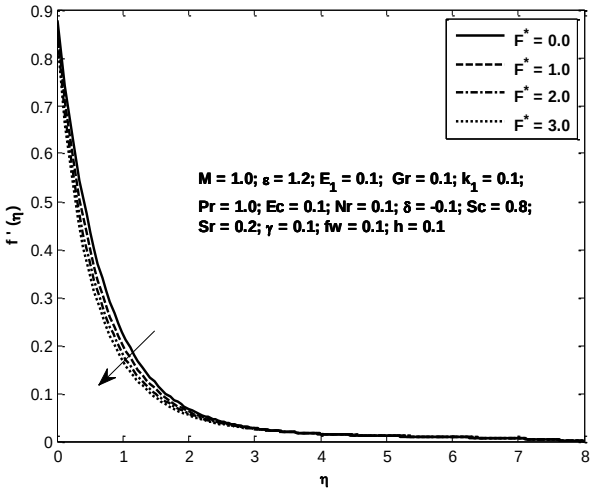


Fig. 11: Velocity profiles for different Values of F^*

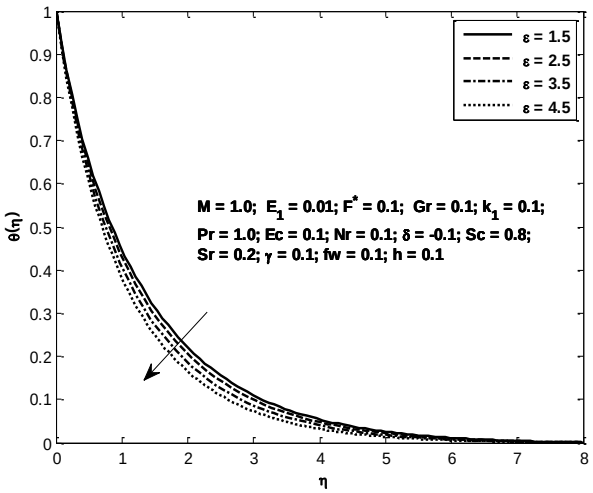


Fig. 9: Temperature profiles for different values of ε

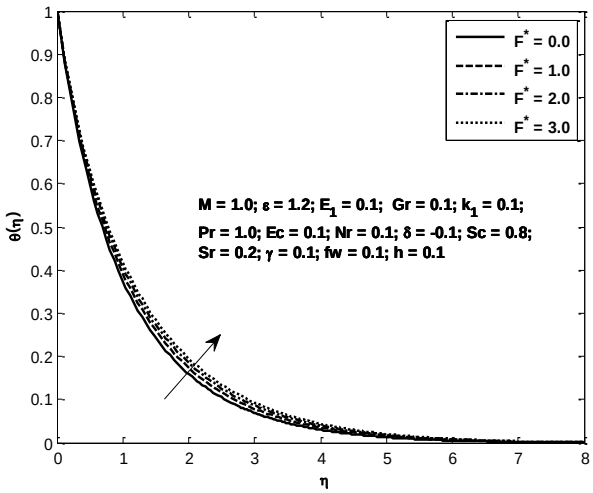


Fig. 12: Temperature profiles for different values of F^*

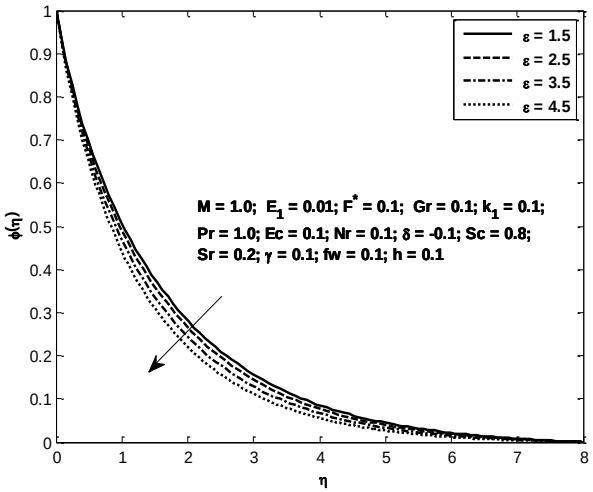


Fig. 10: Concentration profiles for different values of ε

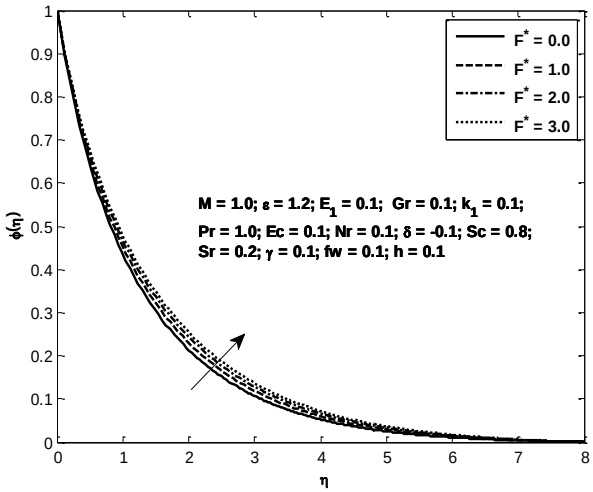


Fig. 13: Concentration profiles for different values of F^*

International Journal of Engineering Applied Sciences and Technology, 2016
Vol. 1, Issue 6, ISSN No. 2455-2143, Pages 52-62
Published Online April - May 2016 in IJEAST (http://www.ijeast.com)

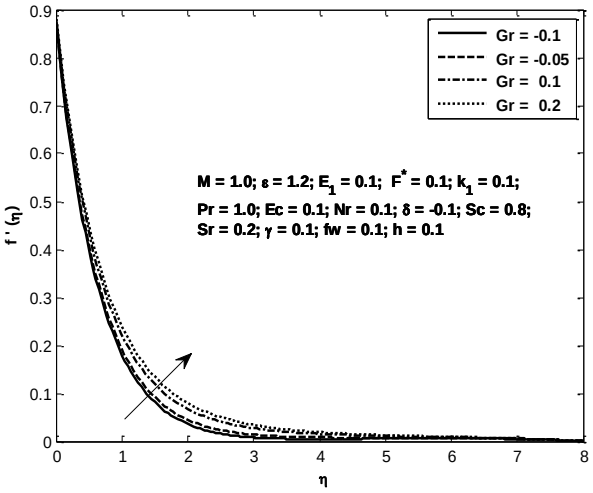


Fig. 14: Velocity profiles for different Values of Gr

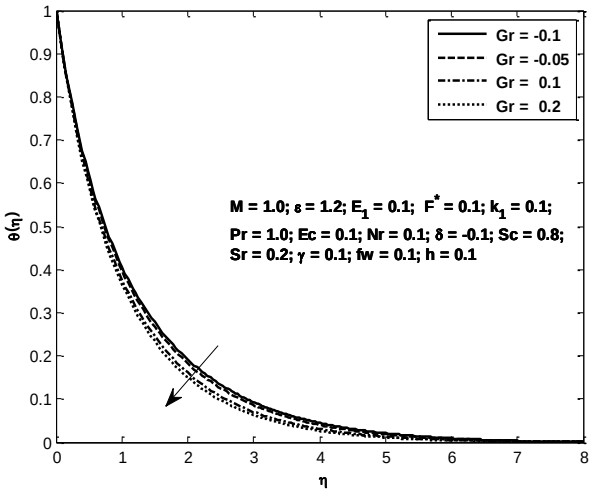


Fig. 15: Temperature profiles for different values of Gr

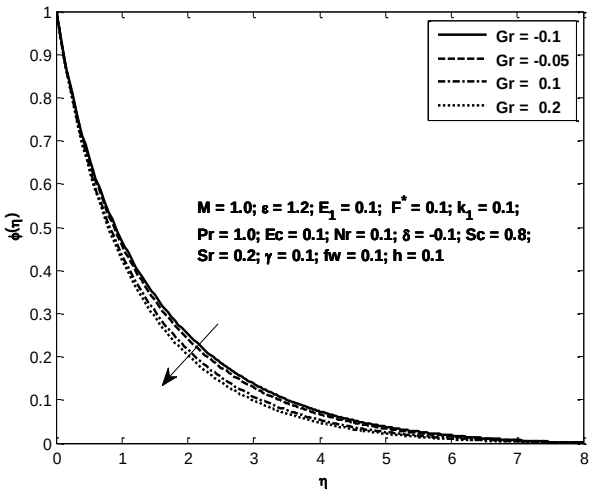


Fig. 16: Concentration profiles for different values of Gr

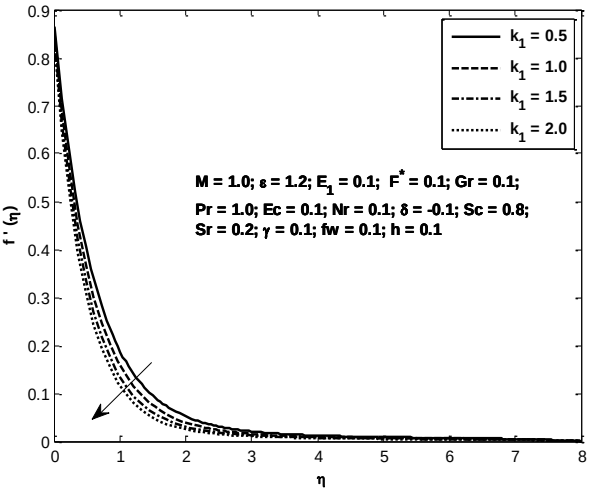


Fig. 17: Velocity profiles for different Values of k_1

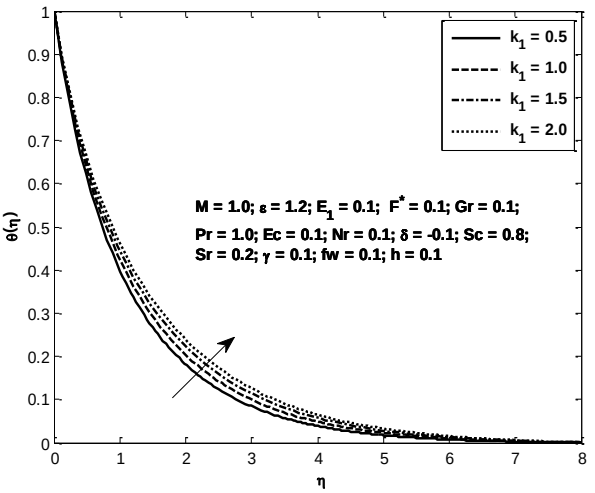


Fig. 18: Temperature profiles for different values of k_1

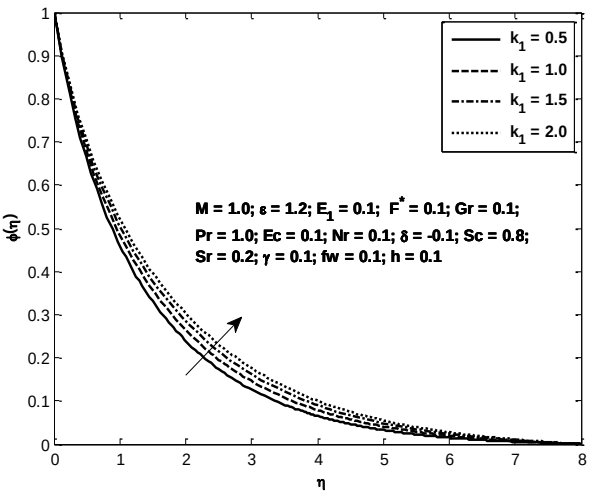


Fig. 19: Concentration profiles for different values of k_1

International Journal of Engineering Applied Sciences and Technology, 2016
Vol. 1, Issue 6, ISSN No. 2455-2143, Pages 52-62
Published Online April - May 2016 in IJEAST (http://www.ijeast.com)

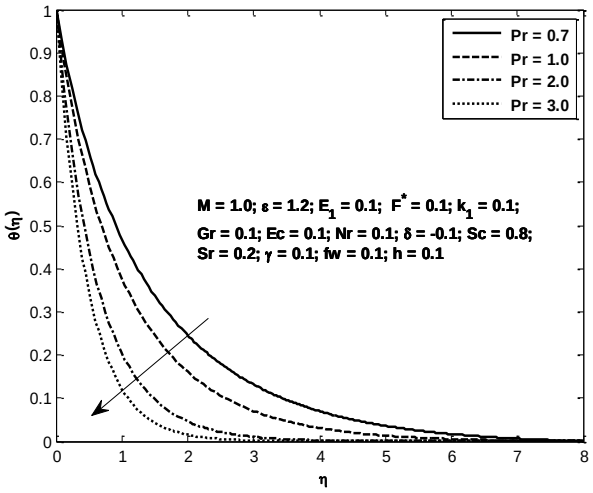


Fig. 20: Temperature profiles for different values of Pr

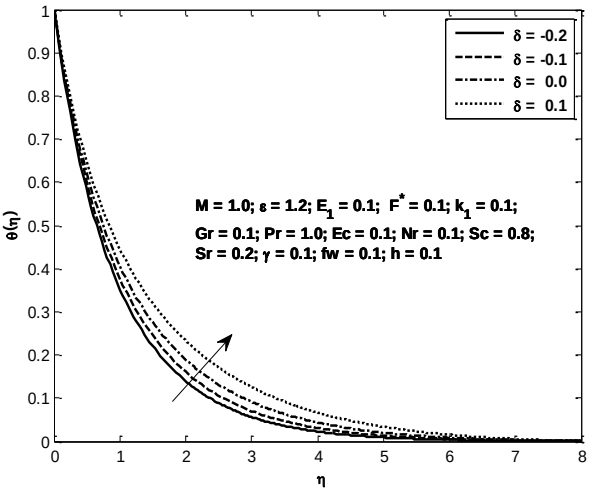


Fig. 23: Temperature profiles for different values of δ

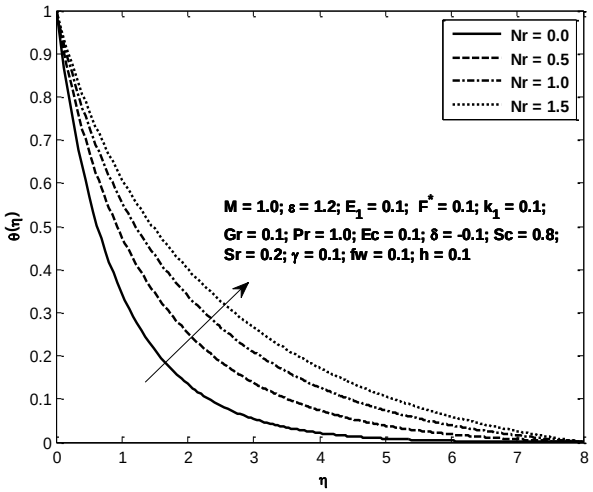


Fig. 21: Temperature profiles for different values of Nr

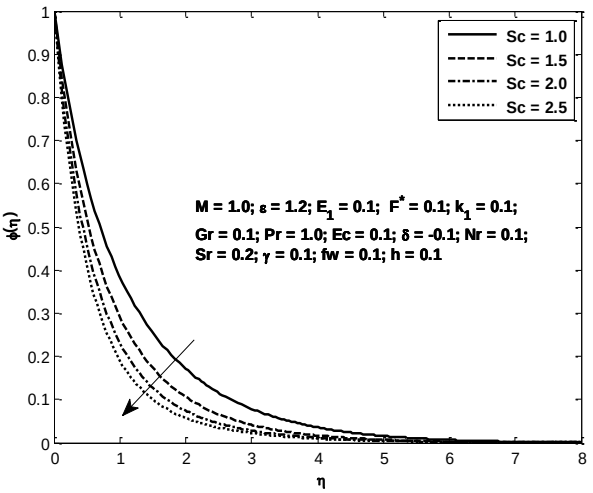


Fig. 24: Concentration profiles for different values of Sc

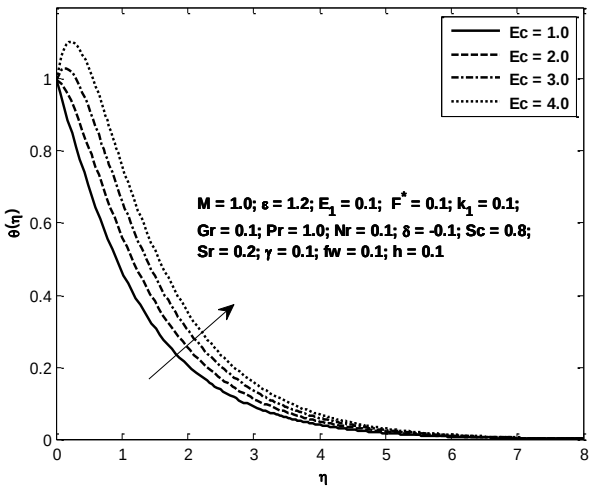


Fig. 22: Temperature profiles for different values of Ec

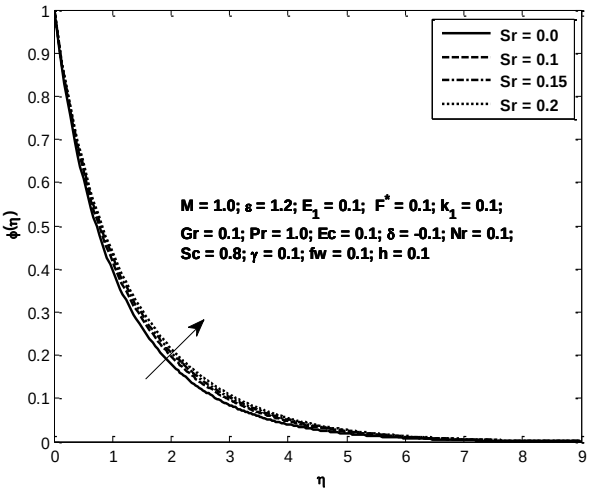


Fig. 25: Concentration profiles for different values of Sr

International Journal of Engineering Applied Sciences and Technology, 2016
Vol. 1, Issue 6, ISSN No. 2455-2143, Pages 52-62
Published Online April - May 2016 in IJEAST (http://www.ijeast.com)

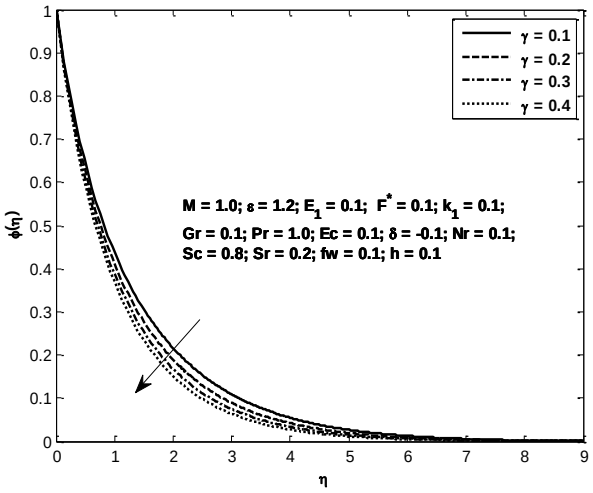


Fig. 26: Concentration profiles for different values of γ

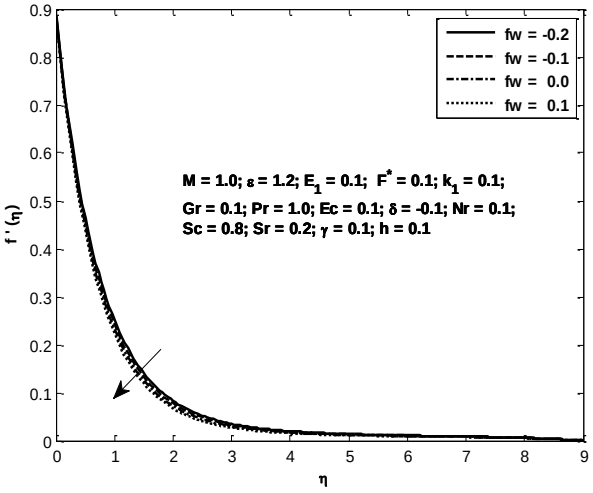


Fig. 27: Velocity profiles for different Values of fw

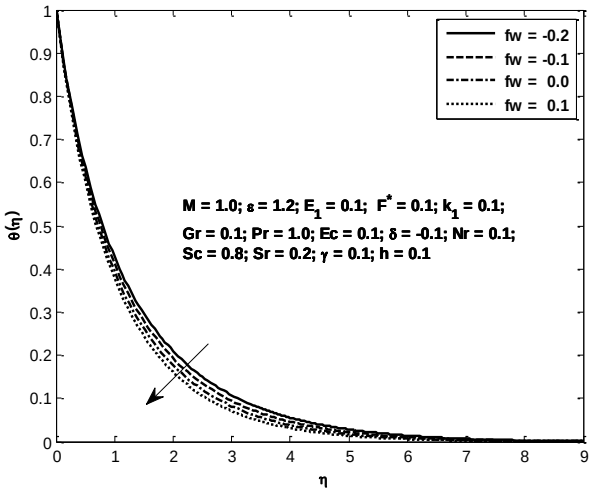


Fig. 28: Temperature profiles for different values of fw

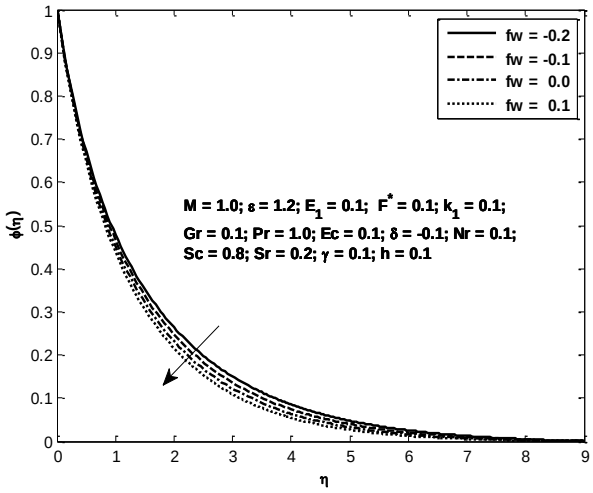


Fig. 29: Concentration profiles for different values of fw

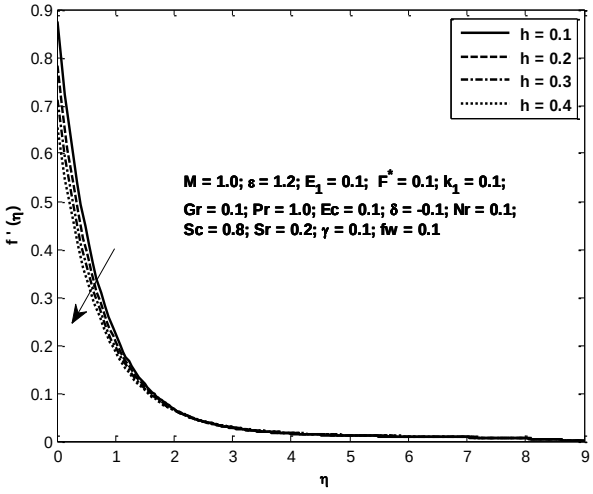


Fig. 30: Velocity profiles for different Values of h

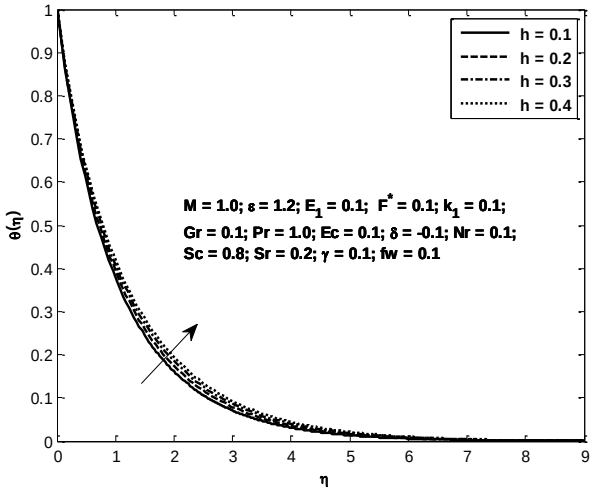


Fig. 31: Temperature profiles for different values of h

International Journal of Engineering Applied Sciences and Technology, 2016
Vol. 1, Issue 6, ISSN No. 2455-2143, Pages 52-62
Published Online April - May 2016 in IJEAST (http://www.ijeast.com)

Table -2 Skin friction coefficient, Nusselt number and Sherwood number for various values of pertinent parameters

M	E_1	F^*	Gr	k_1	Pr	Nr	Ec	δ	Sc	γ	Sr	fw	h	$f''(0)$	$-\theta'(0)$	$-\phi'(0)$
1.0 2.0 3.0 4.0	1.0	0.1	0.1	0.1	1.0	0.1	0.1	-0.1	0.8	0.1	0.2	0.1	0.1	-0.536210 -0.425394 -0.360600 -0.316554	1.426660 1.465449 1.486832 1.500606	1.239496 1.273960 1.292111 1.303714
1.0	0.01 0.04 0.07 0.1	0.1	0.1	0.1	1.0	0.1	0.1	-0.1	0.8	0.1	0.2	0.1	0.1	-1.246928 -1.223531 -1.200230 -1.177049	1.094762 1.114864 1.133197 1.150153	0.962433 0.979523 0.994816 1.008749
1.0	1.0	0.0 1.0 2.0 3.0	0.1	0.1	1.0	0.1	0.1	-0.1	0.8	0.1	0.2	0.1	0.1	-0.496076 -0.823966 -1.049791 -1.226008	1.436198 1.341402 1.274731 1.222617	1.248281 1.176359 1.128341 1.091942
1.0	1.0	0.1	-0.1 -0.05 0.1 0.2	0.1	1.0	0.1	0.1	-0.1	0.8	0.1	0.2	0.1	0.1	-0.605800 -0.588487 -0.536946 -0.502907	1.409392 1.413265 1.424615 1.431965	1.227304 1.230322 1.239214 1.245014
1.0	1.0	0.1	0.1	0.5 1.0 1.5 2.0	1.0	0.1	0.1	-0.1	0.8	0.1	0.2	0.1	0.1	-0.724342 -0.922127 -1.090054 -1.235966	1.363812 1.294543 1.232182 1.175878	1.193255 1.143392 1.100348 1.062738
1.0	1.0	0.1	0.1	0.1	0.7 1.0 2.0 3.0	0.1	0.1	-0.1	0.8	0.1	0.2	0.1	0.1	-0.537195 -0.536946 -0.536412 -0.536081	1.174751 1.424615 2.074913 2.588140	1.269700 1.239214 1.153588 1.081860
1.0	1.0	0.1	0.1	0.1	1.0	0.5 1.0 1.5 2.0	0.1	-0.1	0.8	0.1	0.2	0.1	0.1	-0.536854 -0.537214 -0.537423 -0.537564	1.524504 1.156502 0.964509 0.842404	1.226581 1.271855 1.293817 1.307005
1.0	1.0	0.1	0.1	0.1	1.0	0.1	1.0 2.0 3.0 4.0	-0.1	0.8	0.1	0.2	0.1	0.1	-0.537083 -0.537234 -0.537386 -0.537539	1.290280 1.140785 0.991042 0.841049	1.250017 1.262039 1.274079 1.286139
1.0	1.0	0.1	0.1	0.1	1.0	0.1	0.1	-0.2 -0.1 0.0 0.1	0.8	0.1	0.2	0.1	0.1	-0.536918 -0.536946 -0.536976 -0.537008	1.457482 1.424615 1.390851 1.356110	1.235022 1.239214 1.243495 1.247869
1.0	1.0	0.1	0.1	0.1	1.0	0.1	0.1	-0.1	1.0 1.5 2.0 2.5	0.1	0.2	0.1	0.1	-0.538766 -0.542011 -0.544233 -0.545894	1.423977 1.422902 1.422216 1.421732	1.390010 1.713752 1.989666 2.235106
1.0	1.0	0.1	0.1	0.1	1.0	0.1	0.1	-0.1	0.8	0.1 0.2 0.3 0.4	0.2	0.1	0.1	-0.536483 -0.536844 -0.537191 -0.537523	1.425176 1.425052 1.424934 1.424822	1.239458 1.271723 1.303213 1.333980
1.0	1.0	0.1	0.1	0.1	1.0	0.1	0.1	-0.1	0.8	0.1	0.0 0.1 0.15 2.0	0.1	0.1	-0.537969 -0.537226 -0.536854 -0.536483	1.424660 1.424918 1.425047 1.425176	1.365095 1.302284 1.270873 1.239458
1.0	1.0	0.1	0.1	0.1	1.0	0.1	0.1	-0.1	0.8	0.1	0.2	-0.2 -0.1 0.0 0.1	0.1	-0.501201 -0.512741 -0.524503 -0.536483	1.291053 1.334424 1.379136 1.425176	1.137852 1.170839 1.204710 1.239458
1.0	1.0	0.1	0.1	0.1	1.0	0.1	0.1	-0.1	0.8	0.1	0.2	0.1	0.1 0.2 0.3 0.4	-0.536483 -0.463135 -0.407765 -0.364403	1.425176 1.407092 1.393010 1.381716	1.239458 1.223663 1.211552 1.201950

International Journal of Engineering Applied Sciences and Technology, 2015
Vol. 1, No. 1, Pages 1-6
Published Online June – July 2015 in IJEAST (http://www.ijeast.com)

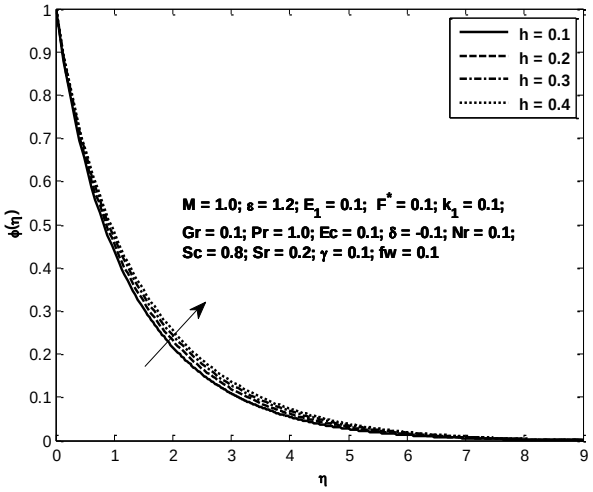


Fig. 32: Concentration profiles for different values of h

IV. CONCLUSION

In this paper, we studied the effect of Soret, electrical field, thermal radiation and mixed convective non-Darcy flow over a permeable stretching surface under the influence of a magnetic field. The features of the flow characteristics are analyzed and discussed in detail through the graphical plots. The salient features are summarized as follows:

- The boundary layer flow attains for stronger magnetic field.
- The electrical force accelerated the flow giving rise to higher velocities and the thickness of the thermal boundary layers is reduced.
- The inertial parameter decreased the velocity while temperature and concentration of the fluid are raised.
- The buoyancy force is seen to enhance the velocities and to reduce the thickness of thermal solutal boundary layers.
- The viscous heating and thermal radiation enhanced the temperature.
- The Schmidt number and chemical reaction parameter produced thinner solutal boundary layers with a reduction in concentration.

V. REFERENCE

[1] C. H. Chen, "Laminar mixed convection adjacent to vertical continuously stretching sheets", *Heat and Mass Transfer*, 33, pp. 471 – 476, 1998.

[2] Dulal Pal and Hiranmoy Mondal, " Soret and Dufour effects on MHD non-Darcian mixed convection heat and mass transfer over a stretching sheet with non-uniform heat source/sink", *Physica B*, 407, pp.642 – 651, 2012.

[3] Dulal Pal and Hiranmoy Mondal, "MHD non-Darcy mixed convective diffusion of species over a stretching sheet embedded in a porous medium with non-uniform heat source/sink, variable viscosity and Soret effect", *Commun Nonlinear Sci Numer Simular*, 17, pp. 672 – 684, 2012.

[4] G. M. Reddy and B. N. Reddy, "Soret and Dufour effects on steady MHD free convection flow past a semi infinite moving vertical plate in a porous medium with viscous dissipation", Int. J. Appl. Math. Mech., 6(1), pp.1 – 12, 2010.

[5] L. J. Grubka and K. M. Bobba, "Heat transfer characteristics of a continuous stretching surface with variable temperature", *ASME J. Heat Transfer*, 107, pp. 248 – 250, 1985.

[6] M. A. E. Aziz, "Flow and heat transfer over an unsteady stretching surface with Hall effect", *Meccanica*, 45, pp. 97 – 109, 2010.

[7] M. V. Karwe and B. Jaluria, "Numerical simulation of thermal transport associated with a continuously moving flat sheet in material processing", *ASME J. Heat Transf.*, 113, pp. 612 – 619, 1991.

[8] P. Sing and K. Tewari, "Non-Darcy free convection from vertical surfaces in thermally stratified porous medium", *Int. J. Eng. Sci.*, 31, pp. 1233 – 1242, 1993.

[9] P. V. S. N. Murthy, Ch. RamReddy, A. J. Chamkha, A. M. Rashad, "Magnetic effect on thermally stratified nano fluid saturated non-Darcy porous medium under convective boundary condition", International Communications in Heat and Mass Transfer, 47, pp. 41 – 48, 2013.

[10] S. R. Vempati and A. B. Laxmi-Narayana-Gari, "Soret and Dufour effects on unsteady MHD flow past an infinite vertical porous plate with thermal radiation", Appl. Math. Mech. Engl. Ed., 31 (12), pp. 1481 – 1496, 2010.

IJEAST

INTERNATIONAL JOURNAL
OF ENGINEERING APPLIED SCIENCE AND TECHNOLOGY

AUTHORS

- Kalyani Ch
- Sreelakshmi
- K Sarojamma G

ABOUT IJEAST

International journal of Engineering Applied Science and Technology (IJEAST) is a peer-reviewed, open access journal that publishes high - quality research paper in the field of Engineering, Applied Science and Technology.

IJEAST aims to provide a platform for researchers, academicians, and professionals to share their innovative ideas, research findings, and practical experiences with the global scientific community.

JOURNAL METRICS

H-INDEX	i10-INDEX	IJEAST CITATIONS	PEER-REVIEWED & OPEN ACCESS
33	154	9,647 (IJEAST CITATIONS)	PUBLISHED MONTHLY

PEER REVIEWED

All submission are rigorously peer reviewed to ensure quality.

AUTHORS ARE OUR PRIORITY

We value our authors and recognize their contribution to the advancement of research and knowledge.

OPEN ACCESS

Free and unrestricted access to research for all.

GLOBAL REACH

Connecting researchers and professionals worldwide.

TIMELY PUBLICATION

We ensure a swift and efficient publication process.

For more information, visit our website
www.ijeast.com

editor@ijeast.com
www.ijeast.com
India

2455-2143